$^{40}Ar/^{39}Ar$ Geochronology, Vent Migration, and Hazard Implications of the Youngest Eruptions in the Raton-Clayton Volcanic Field

Matthew J. Zimmerer
2019, pp. 151-160. https://doi.org/10.56577/FFC-70.151
Supplemental data: https://nmgs.nmt.edu/repository/index.cfml?rid=2019003

in:
Geology of the Raton-Clayton Area, Ramos, Frank; Zimmerer, Matthew J.; Zeigler, Kate; Ulmer-Scholle, Dana, New Mexico Geological Society 70 th Annual Fall Field Conference Guidebook, 168 p. https://doi.org/10.56577/FFC-70

This page is intentionally left blank to maintain order of facing pages.

New Mexico Geological Society Guidebook, 70th Field Conference, Geology of the Raton-Clayton Area, 2019, p. 151-160.

^{40}AR/^{39}AR GEOCHRONOLOGY, VENT MIGRATION PATTERNS, AND HAZARD IMPLICATIONS OF THE YOUNGEST ERUPTIONS IN THE RATON-CLAYTON VOLCANIC FIELD

Matthew J. Zimmerer

New Mexico Bureau of Geology and Mineral Resources, 801 Leroy Pl, Socorro, NM 87801, matthew.zimmerer@nmt.edu

Abstract — Twenty-seven new ^{40}Ar/^{39}Ar ages provide insight into the timing of ten eruptions in the Raton-Clayton volcanic field. The new ages were determined using the high-sensitivity, multi-collector ARGUS VI mass spectrometer. The ARGUS VI yields an increase in analytical precision compared to older generation mass spectrometers, providing an opportunity to re-assess the youngest eruptions in the field. New ages indicate that nine vents erupted between 368.2±7.3 and 36.6±6.0 ka. The average eruption frequency during this pulse of activity is 1 event per 37 ky. However, repose periods between successive eruptions are highly irregular, ranging too short to measure (i.e., statistically indistinguishable ages) to as much as 130 ky. The five youngest eruptions yield ages between 61.7±1.1 and 36.6±6.0 ka and an average recurrence rate of 1 event per 5 ky, indicating an increase in activity during the late Quaternary. The new ages, combined with published geochronology, reveal a previously unrecognized vent migration pattern in this volcanic field. Beginning at approximately 1.3 Ma, the location of volcanic vents has migrated at a rate of 2.3 cm/yr to the east from an area south of Raton to near Capulin Volcano National Monument. Rates of volcanism and vent migration patterns provide fundamentally important temporal-spatial information should the Raton-Clayon volcanic field enter a new period of eruptive activity.

INTRODUCTION

Ongoing research during the past several years is investigating the geochronology of late Quaternary volcanism (i.e., <500 ka) within the Rio Grande rift and along the Jemez lineament to establish eruption frequencies, vent migration patterns, and related volcanic hazards. Previous work (Baldwin and Muehlberger, 1959; Stroud, 1997; Nereson et al., 2013) in the Raton-Clayton volcanic field (RCVF) indicates multiple eruptions during the late Quaternary (Fig. 1). However, the existing geochronology for the RCVF, largely established by Stroud (1997) and further refined by Nereson et al. (2013), is insufficiently precise to document the duration of the eruption cycles and the associated repose periods for many of the late Quaternary volcanic pulses. One of the main motivating factors that initiated this statewide assessment of young volcanism in the rift and lineament was the acquisition of the ARGUS VI mass spectrometer in 2010 at the New Mexico Geochronology Research Laboratory (NMGRL). The ARGUS VI mass spectrometer is a low-volume, high-sensitivity, multi-collector noble gas mass spectrometer capable of routinely producing dates an order of magnitude more precise (Fig. 2) than single-detector mass spectrometers, such as the one previously used to establish the volcanic history of the RCVF (Stroud, 1997). With this increase in analytical capabilities, the youngest pulse of activity in the RCVF was re-investigated to more confidently establish the eruption history and the implications

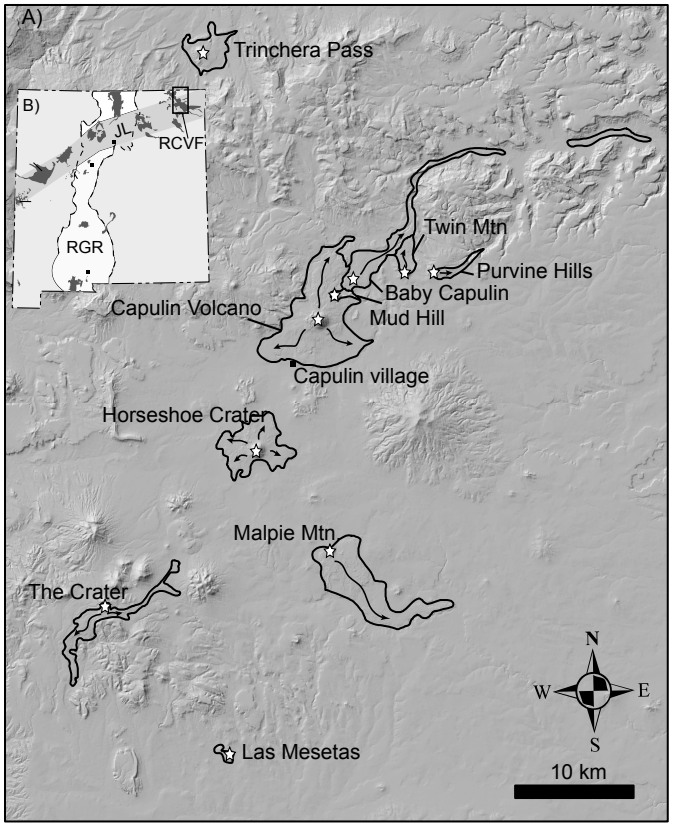

FIGURE 1. **A**) Simplified map showing the locations of the dated eruptive centers in this study. Stars represent the vents. Solid black line outlines the extent of the associated lava flow(s). Arrows show the approximate path of the lava flows. Sample locations are found in the supplementary material. **B**) Inset map shows the location the late Cenozoic volcanic fields within the Rio Grande rift (RGR) and along the Jemez lineament (JL). Raton-Clayton volcanic field (RCVF) is at the NE limits of the lineament. Box over the Raton-Clayton volcanic field (RCVF) is the approximate extent of map A.

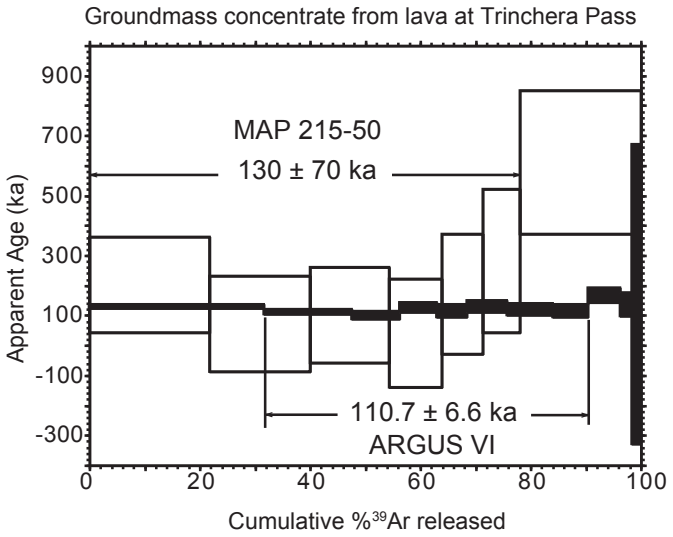

FIGURE 2. Age spectra showing the comparison of the step-heat results for late Quaternary groundmass concentrate dated by the older-generation single-detector MAP 215-50 mass spectrometer versus the newer-generation mutli-collector ARGUS VI mass spectrometer. Individual steps and the plateau age from the single-detector MAP 215-50 mass spectrometer (open symbols) have larger uncertainties than those of the ARGUS VI mass spectrometer (solid black symbols). Data is from the Trinchera Pass eruptive center of the Raton-Clayton volcanic field. MAP 215-50 data from Stroud (1997). ARGUS VI data from this study. Uncertainties reported at 2-sigma.

for future volcanic activity. This paper presents a preliminary assessment of the results.

GEOLOGIC FRAMEWORK

Late Cenozoic volcanism (e.g., <10 Ma) in New Mexico is widespread, but is concentrated within the Rio Grande rift and along the Jemez lineament. Volcanic vents active during this period cluster into about 9 major volcanic fields (fields with an areal extent more than ~1000 km^2; Fig. 1B) and several numerous isolated vents (e.g., Jornada del Muerto volcano; Hoffer and Corbitt, 1991) and fissure systems (e.g., Cat Hills; Kelly and Kudo, 1978). The RCVF is located at the northeastern terminus of the Jemez lineament, an NE-trending zone of apparent crustal weakness (Karlstrom and Bowring, 1988) that concentrated magmatism and eruptions for at least the last 10 Ma (Chapin, 2004). Some volcanic fields within the rift and along the lineament have protracted volcanic histories greater than several My (e.g., >5 My duration at the Taos Plateau volcanic field; Appelt 1998), whereas other fields have much shorter lifespans and have only been active during the last 1 Ma (e.g., Potrillo volcanic field; William, 1999).

The Raton-Clayton volcanic field is one of the longest-lived and the largest volcanic field along the Jemez lineament. Volcanic outcrops in the field cover an area of approximately 20,000 km^2. The majority of the field is located in New Mexico, but a few eruptive centers and flows are located in southern Colorado. Volcanic activity in the field began as early as 9.2 Ma and continued throughout the late Quaternary (Stroud, 1997). Regional maps (Scholle, 2003) indicate as many as 142 vents within the field. However, the total number of eruptions may be less than the total number of vents because some of the eruptive centers, particularly in the southern part of the field, form alignments suggestive of monogenetic fissure eruptions (i.e., a single eruption from multiple cones rather than a single vent). Regardless, activity in the field constitutes one of the largest magmatic flare-ups along the lineament during the late Cenozoic.

In addition to the long-duration of activity in the RCVF, lavas in the field are characterized by significant compositional diversity. Early research in the field grouped the volcanic eruptions into three phases based largely on composition, geographic location, and K-Ar ages (Baldwin and Muehlberger, 1959; Stormer, 1972). Subsequent investigations using the $^{40}Ar/^{39}Ar$ technique (Stroud, 1997; Nereson et al., 2011) further refined the timing of these events. The Raton phase (9.2-3.5 Ma) is the earliest pulse of volcanism in the field and the most compositionally diverse. The majority of the vents active during the Raton phase are located in the western-half of the field and include the most southern and northern clusters of eruptive centers. Most of the eruptions during this phase are alkali olivine basalt, although silicic composition such as trachyte, rhyolite, rhyodacite, and dacites (Stormer, 1972; Scott et al., 1990) are present. During the Clayton phase (3.0-2.2 Ma), volcanism shifted to the eastern sector of the field. Eruptions during this period are dominantly olivine basalts. The final phase of activity (<1.7 Ma) is known as the Capulin phase. Vents active during this period are located south of Raton and near the village of Capulin in the center of the field. Olivine-bearing basalts and smaller-volumes of basaltic andesites characterize this last pulse of activity (Baldwin and Muehlberger, 1959; Stormer, 1972).

Of particular relevance for this study, previous work (Stroud, 1997; Nereson et al., 2013) indicates low to moderate eruptive activity during the late Quaternary. Seven vents yielded $^{40}Ar/^{39}Ar$ ages that, within uncertainty, are less than 500 ka. Ages group into three pulses at ~ 450 ka (n = 3 eruptions), ~125 ka (n = 2 eruptions), and ~55 ka (n = 2 eruptions). Ages of individual vents within each of these three pulses of activity have uncertainties ranging from ±8 to 200 ka and are commonly statistically indistinguishable from the next oldest or youngest center that define each pulse. Thus, the eruption frequency and repose period between the eruptions, two common parameters used to classify the activity of the volcanic field, were neither determined, nor was it a primary goal of the previous work.

METHODS

Sample collection was guided, in part, by the previous $^{40}Ar/^{39}Ar$ geochronology of Stroud (1997) that indicates late Quaternary volcanism in the RCVF. Samples of Baby Capulin volcano, which was not dated until this study, were collected because stratigraphic relationships indicate that this vent is younger than the well-dated 56 ka Capulin flow (Baldwin and Muehlberger, 1959; Sayre and Ort, 2011). Aerial images indicate Malpie Mountain, also not dated until this study, displays a similar flow morphology (e.g., well-defined pressure ridges on the poorly vegetated flow surfaces) to the flows of Capulin Volcano. Thus samples of Malpie Mountain were also collected. Mud Hill volcano, located north of Capulin Volca-

no, and although being demonstrably older and more eroded than Capulin, had not been previously dated and a sample was collected for geochronology and completeness for this study. Because of the young age and limited erosion of the majority of the centers, well-crystallized interiors of the flows were typically not well exposed for sampling. Samples were collected from the densest, most crystalline exposed parts of the flows. Glassy flow surfaces or samples with abundant secondary minerals within vesicles were avoided when possible.

^{40}Ar/^{39}Ar dating was completed at the NMGRL. Groundmass was concentrated using standard separation techniques designed to remove phenocrysts and any $CaCO_3$ from the groundmass. Samples were irradiated with the 28.201 Ma FC-2 interlaboratory standard (Kuiper et al., 2008) to monitor neutron flux. Samples were incrementally degassed using a defocused 810-nm diode laser. Sample gas was cleaned in an all-metal, fully-automated extraction line. Most isotopic ratios were measured with the ARGUS VI mass spectrometer. In October 2016, the NMGRL acquired the Thermo Helix MC Plus, a high-resolution, multi-collector mass spectrometer. Two samples were re-dated with this mass spectrometer. Complete analytical details are provided in the supplementary material.

Vent migration patterns were determined by comparing the ^{40}Ar/^{39}Ar ages to the locations of vents. Vent locations were determined from Google Earth. In addition to the samples dated as part of this study, additional samples from Stroud (1997) were used to define migration patterns. For many of the Stroud (1997) samples, the vent was easily identified on Google Earth. For a few samples, however, the vents were not easily identified and thus the sample location, rather than the vent, was used for the spatial analysis. Most of the flows with questionable vent locations have limited areal extent, which did not significantly impact the migration calculations.

RESULTS

^{40}Ar/^{39}Ar ages

Representative age spectra, along with K/Ca and radiogenic yield (%^{40}Ar*) auxiliary plots, are shown in Figure 3. Table 1 is a summary of results. Data tables, spectra, and

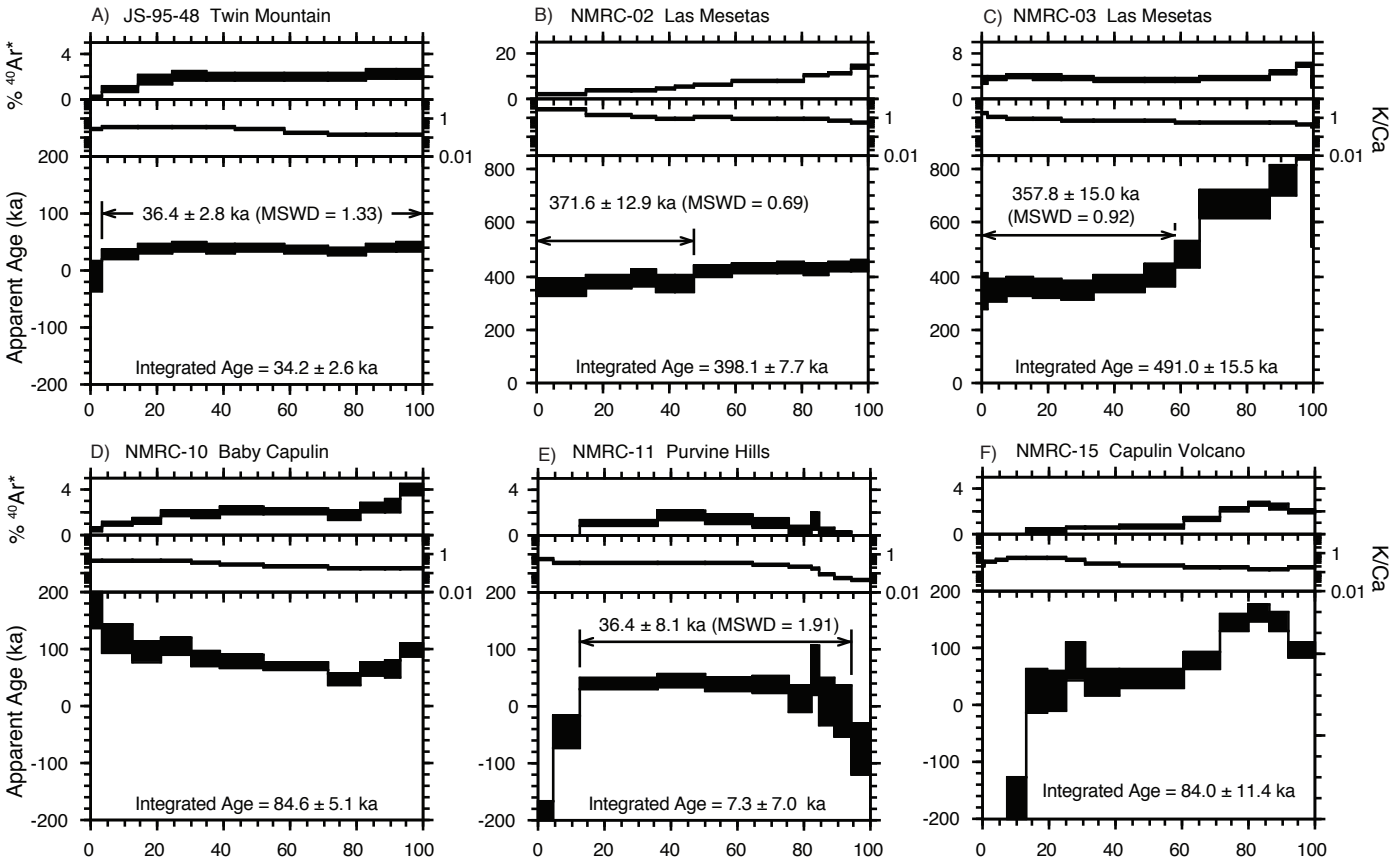

FIGURE 3. Representative groundmass concentrate age spectra showing ^{40}Ar/^{39}Ar results of the late Quaternary centers in the Raton-Clayton volcanic field. Auxiliary plots include K/Ca and radiogenic yield (%^{40}Ar*). Note that the apparent age and % ^{40}Ar* scales are different for some samples. Samples display a variety of complexities. **A**) Spectrum where most of the gas released (>95%) is included in the plateau calculation. **B**) Spectrum where steps define two flat segments. In this case, the younger flat segment composed of ~48% of the gas was preferred to the older, segment composed of 52% of the gas. **C**) Spectrum where the low-temperature steps yield a plateau and the high-temperature steps yield monotonically increasing older ages. Old ages are related to xenocrysts. **D**) Spectrum that did not yield a plateau. This spectrum displays a "U-shaped" profile typical of samples that contain excess ^{40}Ar. For this sample, the preferred age was calculated from the inverse isochron. **E**) Spectrum where low-temperature steps increase in age (from less than 0 ka), moderate temperature steps yield a plateau, and high temperature steps decrease in age. For spectra with these characteristics, the plateau age is considered a minimum age. **F**) Spectrum with extreme discordance. None of the gas released is of an appropriate age for this sample.

TABLE 1. Summary of $^{40}Ar/^{39}Ar$ ages of this study.

Unit	Sample	Method[a]	MSWD[b]	n[c]	Age (ka) ± 2σ[d]	Eruption Age (ka) ± 2σ[e]
Purvine Hills	NMRC-11	Plateau	1.91	8	36.4 ± 8.1	Weighted Mean
	NMRC-11	Plateau	1.58	8	32.6 ± 6.1	36.6 ± 6.0
	NMRC-11	Plateau	1.06	6	42.7 ± 7.5	
Twin Mountain	JS-95-48	Plateau	1.47	9	42.6 ± 11.4	Weighted Mean
	JS-95-48	Plateau	1.33	9	36.4 ± 2.8	36.7 ± 2.3
	JS-95-48	Plateau	1.88	7	37.4 ± 4.2	
Baby Capulin	NMRC-10	Isochron	0.41	7	51.7 ± 9.9	Weighted Mean
	NMRC-17A	Plateau	2.25	4	48.2 ± 8.5	44.8 ± 2.2
	NMRC-17B	Plateau	2.39	7	43.1 ± 2.9	
	NMRC-17B	Plateau	0.87	5	45.9 ± 2.6	
Capulin	NMRC-13	Plateau	3.89	7	54.2 ± 4.8	Weighted Mean
	NMRC-16	Plateau	0.44	8	54.2 ± 1.9	54.2 ± 1.8
Malpie Mtn	NMRC-23	Plateau	3.65	4	64.2 ± 2.3	Weighted Mean
	NMRC-23	Plateau	1.94	4	61.5 ± 0.7	61.7 ± 1.1
	NMRC-24	Isochron	3.4	8	60.6 ± 19.2	
The Crater	NMRC-04	Plateau	2.14	9	101.6 ± 4.9	Weighted Mean
	NMRC-05	Plateau	1.41	5	96.1 ± 3.2	97.7 ± 5.0
Trinchera Pass	NMRC-09	Isochron	7.8	7	117.1 ± 10.5	Weighted Mean
	NMRC-09	Plateau	1.36	7	110.7 ± 6.6	112.5 ± 5.8
Horseshoe Crater	NMRC-06	Isochron	4.56	6	242.2 ± 7.7	Weighted Mean
	NMRC-06	Isochron	0.83	6	238.9 ± 16.4	238.2 ± 6.4
	NMRC-07	Isochron	3.9	6	232.5 ± 9	
Las Mesetas	NMRC-02	Isochron	3.9	6	370.3 ± 9.3	Weighted Mean
	NMRC-02	Plateau	0.69	8	371.6 ± 12.9	368.2 ± 7.3
	NMRC-03	Plateau	0.92	7	357.8 ± 15.3	
	NMRC-03	Isochron	80.95	11	*217 ± 13.4*	
Mud Hill	NMRC-20	Isochron	2.46	9	1692 ± 32.4	1692 ± 32.4

a – Method used to calculate the age. Plateau method of Fleck et al., (1977). Inverse isochron method of York (1969). See footnote of Table 1 in the supplemental material for more information.
b – Mean square of weighted deviates (MSWD).
c – Number of steps used to calculate the plateau or isochron age.
d – All ages are relative to FC-2 equal to 28.201 Ma (Kuiper et al., 2008). Error includes analytical uncertainties, error in the J measurement, and error in the correction factors.
e – Eruption age is calculated from the weighted mean of the individual ages in the previous column. Age in italics was not used in this calculation.

inverse isochron plots for all 31 dated samples are in Data Repository 20190001. Plateau ages, integrated ages, and inverse isochron ages are reported at 2σ and include analytical and irradiation uncertainties. A plateau is defined as three or more contiguous steps that overlap at 2σ and include ~50% of the gas released (Fleck et al., 1977). Step-heat data was plotted on inverse isochrons to assess excess ^{40}Ar. If the $^{40}Ar/^{36}Ar$ intercept was statistically greater than that of atmosphere (295.5; Nier, 1950), the sample was interpreted to contain excess ^{40}Ar and the inverse isochron age was chosen for the preferred age. When numerous aliquots of a single sample or multiple samples were dated for a single vent or flow, the preferred eruption age was determined by calculating an inverse variance weighted mean of all available data (Table 1 and data of Fig. 4).

Of the 31 samples dated, 27 samples yield interpretable ages (Table 1). Plateau ages are preferred for 18 samples. The remaining 9 samples contain excess ^{40}Ar and thus, the inverse isochron age is preferred. Four samples yield a spectrum and/or isochron that is too discordant for an age assignment. Despite sample-to-sample variation in the degassing behavior of the groundmass concentrate, most of the samples share similar trends in K/Ca ratios and radiogenic yield. K/Ca values of the low-wattage (i.e., low temperatures) early steps are typically ~1 and decrease to values of ~0.1 during the step-heating experiment. This is interpreted to represent degassing of different

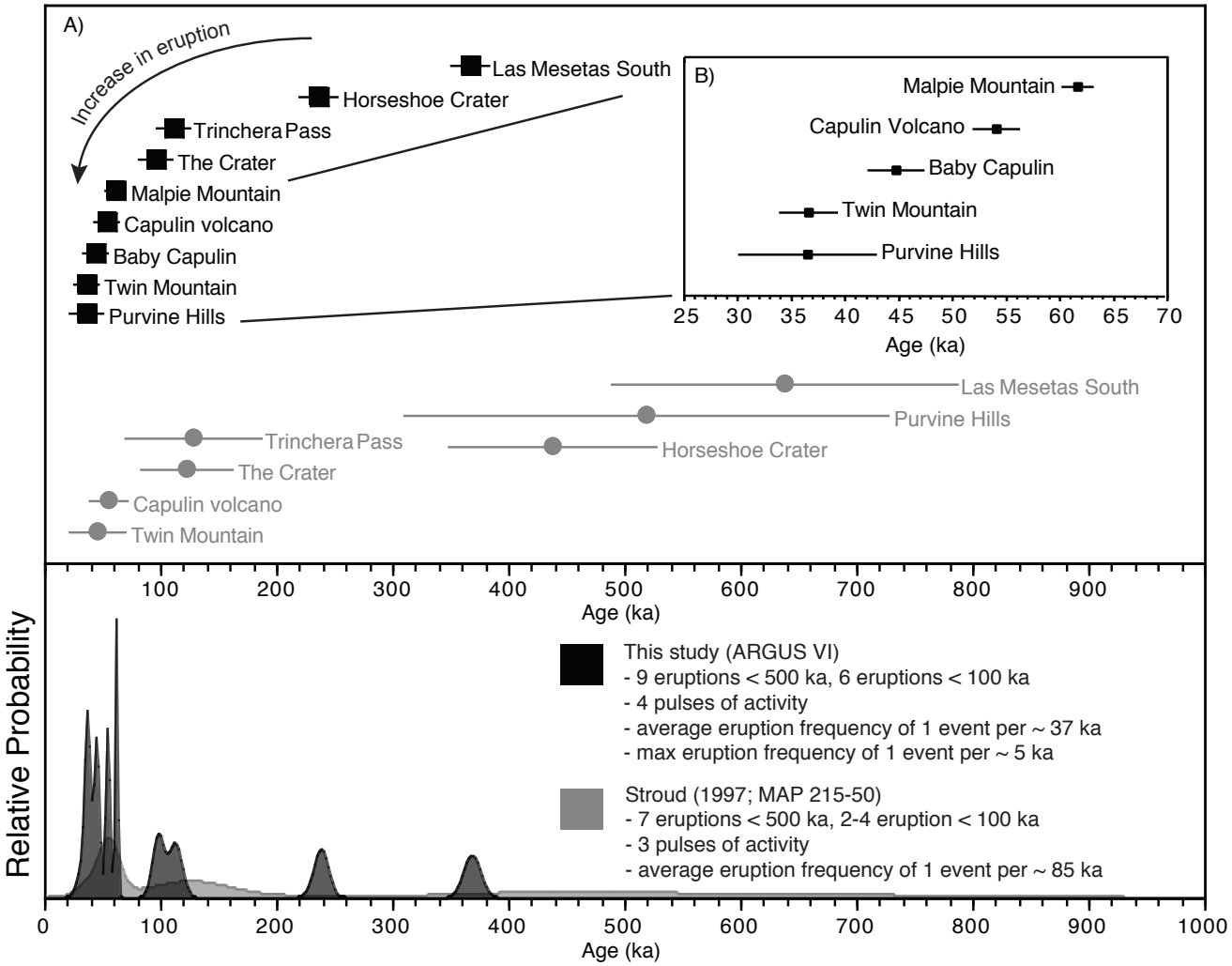

FIGURE 4. Diagrams showing a summary of late Quaternary volcanism in the Raton-Clayton volcanic field. **A**) Comparison of the new ^{40}Ar/^{39}Ar ages (data colored black) to those of Stroud (1997; data colored gray). **B**) Inset shows just the youngest ages from this study. Note the change in scales between graph A and B. Ages and uncertainties reported at 2σ.

phases in the groundmass during the experiment. K-rich glass and interstitial phases preferentially degas at low to moderate temperatures. Ca-rich phases, such as plagioclase and pyroxene, preferentially degas at moderate to high temperatures. Radiogenic yields are somewhat variable but typically increase during the experiment. Older samples are more radiogenic (i.e., ^{40}Ar* >10%) than younger samples (i.e., ^{40}Ar* <5%).

Samples analyzed for this study display a variety of complexities and illustrate the challenges of dating young, K-poor groundmass (Fig. 3). Plateau and isochron ages range from 32.6±6.1 ka to 1692±32.4 ka (Table 1). For most of the late Quaternary samples, the 2σ uncertainty are <10 ka and commonly <5 ka. In general, the most precise ages are from samples that yield a plateau (Fig. 3A, B) or have a range of radiogenic yields so that steps define a line, rather than a cluster, on an inverse isochron. Most samples display some discordance at either the low and/or high temperature steps. Young, low temperature steps are interpreted to represent minor alteration and ^{40}Ar loss of interstitial glass. Old, low temperature steps commonly correlate to the presence of excess ^{40}Ar (Fig. 3D). Old ages at the end of the spectra are likely related to excess ^{40}Ar (Fig. 3D) or degassing of antecrysts/xenocrysts in the groundmass (Fig. 3C). A few spectra contain initial steps with negative ages (Fig. 3E, F). This is interpreted to reflect ^{40}Ar–^{36}Ar fractionation, which results in an over-estimation of the atmospheric ^{40}Ar and thus, an under-estimation of the radiogenic ^{40}Ar. Fractionation is not completely understood at this time, but may happen geologically, during alteration (preferential incorporation of ^{36}Ar relative to ^{40}Ar into glass during hydration), or analytically, during step-heating (preferential degassing of ^{36}Ar relative to ^{40}Ar at low temperatures).

Migration rates

Migration rates (Fig. 5) were determined by plotting the preferred eruption age (i.e., a weighted mean of all available and acceptable data; Table 1) relative to the easting and northing of the source vent (Table 2). The linear regression of age versus easting component of migration yields a migration rate of 2.3 cm/yr and a R^2 value of 0.68 (Fig. 5B). The linear re-

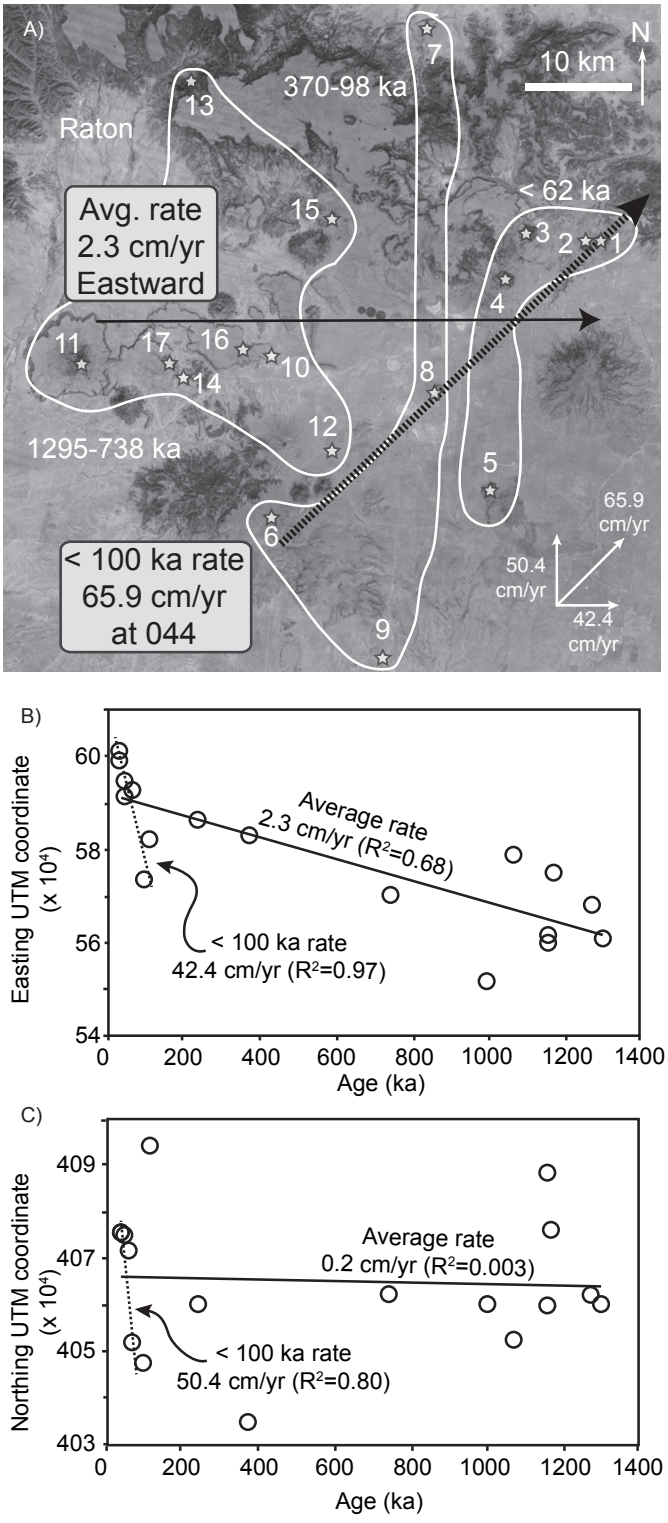

FIGURE 5. Map and diagrams showing vent migration patterns of late Quaternary volcanism in the Raton-Clayton volcanic field. **A**) Simplified map showing the location of the vents (stars) that define the eastward migration of volcanism. White lines outline vents with similar ages. Numbers by each vent correspond to the vent number and name in Table 2. **B**) Diagram showing vent age versus easting indicating an eastward vent migration. Solid line is the linear regression of migration since 1.3 Ma and yields a slope equal to a migration rate of 2.3 cm/yr. The dotted line is the linear regression for only the vents that are <100 ka. **C**) Diagram showing age versus northing indicating no northward vent migration. Solid and dotted lines are the linear regressions for <1.3 Ma and <100 ka vents, respectively.

gression of age versus northing yields a low R^2 value of 0.003 (Fig. 5C), indicating no systematic trend in the change in the latitude of the vents during the last ~1 Ma. Migration patterns calculated for the vents <100 ka yield a net rate of 65.9 cm/yr to the northeast (dotted lines of Fig. 5).

DISCUSSION

Sample Reproducibility and Accuracy

Sample reproducibility and accuracy was tested by analyzing different samples from the same flow, by analyzing different aliquots of the same sample at different times or within different irradiations, and by comparing ages to stratigraphic relationships. For most eruptive centers (e.g., NMRC-11 of Purvine Hills, JS-95-48 of Twin Mountain, both samples of Capulin; Table 1), ages from different samples or multiple aliquots of the same are indistinguishable at the 2σ uncertainties. Likewise, ages agree with stratigraphic relationships. For example, the 54.2±1.8 ka flows of Capulin Volcano are located beneath the 44.8±2.2 ka flows of Baby Capulin. Many of the dated vents, however, are isolated from one another (e.g., Malpie Mountain) and thus there are some limitations to using stratigraphic relationships to test accuracy.

Ages of a few samples and aliquots were not reproducible. For example, replicate analyses of sample NMRC-03 from the Las Mesetas vent yielded a plateau for the first aliquot and a wildly discordant spectrum and isochron for the second aliquot. Likewise, two aliquots of NMRC-09 from the Trinchera Pass vent yielded indistinguishable ages, but only by using different age calculation methods. One aliquot contained excess ^{40}Ar and the inverse isochron age was preferred. The second aliquot did not contain excess ^{40}Ar and the plateau age was preferred. The irreproducibility is likely related to small differences in the dated material, where one multi-milligram aliquot (as many as 100 mg — or 100s to 1000s of grains of groundmass — were used for the youngest samples) may contain phases or phenocrysts that are altered or contain excess ^{40}Ar, which thus produced a discordant spectrum. This demonstrates the challenges of dating young, K-poor samples as well as the value of analyzing multiple samples or aliquots to determine accurate eruption ages of late Quaternary volcanoes.

Late Quaternary eruptive history and hazards of the Raton-Clayton volcanic field

New $^{40}Ar/^{39}Ar$ ages provide insight into the timescales of volcanism within the Raton-Clayton field and along the Jemez lineament. All dated samples in this study yield higher-precision ages compared to the pre-existing geochronology (Stroud, 1997) and permit re-interpretation of the late Quaternary eruptive history of the field (Figs. 4, 5). Although many of the new ages agree with the previous geochronology, albeit more precise, some units (e.g., Las Mesetas, Horseshoe Crater, and Purvine Hills) yield ages that are significantly younger than those previously reported (Stroud, 1997). In addition to higher-precision ages, this study also provides new ages for three

TABLE 2. Vent name, location, and age that define late Quaternary time-space patterns.

Vent[a]	Easting[b]	Northing	Age (ka)[c] ± 2σ
Purvine Hills (1)	601233	4075108	36.6 ± 6.0
Twin Mountain (2)	599456	4075284	36.7 ± 2.3
Baby Capulin (3)	594833	4074806	44.8 ± 2.2
Capulin Volcano (4)	591881	4071195	54.2 ± 1.8 61.7 ± 1.1
Malpai Mountain (5)	592643	4051634	97.7 ± 5.0
The Crater (6)	573485	4047140	112.5 ± 5.8
Trinchera Pass (7)	582089	4094176	238.2 ± 6.4
Horseshow Crater (8)	586477	4060179	368.2 ± 7.3 *738 ± 60*
Las Mesetas Southern Vent (9)	583839	4034563	*992 ± 10*
Blosser Mesa Flow (10)	570340	4062370	*1062 ± 190*
Eagle Tail Mountain (11)	551866	4059937	*1154 ± 160* *1154 ± 120*
Hwy 193 cone (12)	578827	4052250	*1164 ± 180*
Yankee Volcano (13)	560067	4088046	*1265 ± 70*
Red Mtn Flow (14)	561805	4059198	*1295 ± 60*
Chaco Arroyo (15)	575190	4075963	
Blosser Mesa (16)	567766	4062150	
Red Mountain Vent (17)	560926	4060109	

a - Vent locations determined from Google Earth. Number in parentheses corresponds to vent location in Figure 5A.
b - Datum for Easting and Northing is NAD 83. All coordinates in section 13S.
c - Ages in italics are from Stroud (1997) and recalculated relative to FC-2 equal to 28.201 Ma (Kuiper et al., 2008).
All other ages from this study.

previously undated centers (Mud Hill, Malpie Mountain, and Baby Capulin), as well as identifying three vents (Baby Capulin, Twin Mountain, and Purvine Hills) that are younger than Capulin Volcano.

The oldest unit dated in this study is Mud Hill. The inverse isochron age of Mud Hill is 1692±32 ka and is the interpreted eruption age. This age indicates that Mud Hill is one of the oldest eruptive centers of the Capulin pulse. Younger flows of Capulin Volcano bank along the northern flanks of the Mud Hill tuff cone and thus the age of the Mud Hill is consistent with the available stratigraphic constraints. As discussed later, the age and location of Mud Hill provides some insight into the initiation of vent migration.

Dating indicates that nine vents in the Raton-Clayton volcanic field were active during the late Quaternary (Figs. 1, 4; Table 1). Prior to the pulse of activity centered near Capulin Volcano, late Quaternary eruptions in the field occurred mainly as geographically isolated single events with significant repose periods between pulses of activity. Las Mesetas vent, located in the southern reaches of the field, erupted at 368.2±7.2 ka. After an eruptive hiatus of 130 ky, Horseshoe Crater erupted at 238.2±6.4 ka. The next youngest eruption is the cone at Trinchera Pass along the New Mexico–Colorado border, which yields an age of 112.5±5.8 ka. After another hiatus of 14.8±7.7 ky, The Crater erupted at 97.7±5.0 ka in the southern part of the field (north of Las Mesetas and south of Horseshoe Crater). The average eruption frequency during this period was 1 event per ~68 ky (4 events between 368.2 and 97.7 ka), which is similar to the poorly constrained long-term rates of 1 event per 65 ky for the entire field (142 events between 9.2 Ma and 37 ka).

With the exception of Malpie Mountain, the youngest pulse of volcanism in the Raton-Clayton field was centered near Capulin Volcano. After a ~36 ka hiatus in activity since the eruption of The Crater, volcanism re-initiated with the eruption of Malpie Mountain. Three ages from two samples of Malpie Mountain yield a weighted mean age of 61.7±1.1 ka. Two samples of Capulin Volcano yield an eruption age of 54.2±1.8 ka. Previous investigations of Capulin Volcano using ^{40}Ar/^{39}Ar and cosmogenic ^{3}He dating methods yielded ages of 56±8 (Stroud, 1997) and 59±6 ka (Sayre et al., 1995), respectively, which are indistinguishable from the new results of this study. The last three eruptions in the field are located north to northeast of Capulin Volcano and include the 44.8±2.2 ka Baby Capulin cinder cone, the 36.7±2.3 ka Twin Mountain cinder cone, and the 36.6±6.0 ka Purvine Hills. An age for Baby Capulin did not exist prior to this study. This new age is consistant with stratigraphic constraints that indicates that Baby Capulin is younger than Capulin Volcano (Baldwin and Muehlberger, 1959; Sayre and Ort, 2011; this study). Stroud (1997) reported an age of 48 ±14 ka for Twin Mountain, which is indistinguishable from the newly determined age. However, the new age of 36.7±2.3 ka indicates that Twin Mountain is conclusively younger than

both Capulin and Baby Capulin volcanoes. Furthermore, field relationships indicate that flows from Twin Mountain travelled north and ponded in the topographic depression formed by the earlier Baby Capulin flows to the west and bluffs that expose Mesozoic strata to the east. The youngest dated eruption in the field is 36.6±2.3 ka at Purvine Hills. The new $^{40}Ar/^{39}Ar$ age is significantly younger than the previously reported $^{40}Ar/^{39}Ar$ age of 530±200 ka. Although the age of Purvine Hills is statistically indistinguishable from that of Twin Mountain, both Baldwin and Muehlberger (1959) and Sayre and Ort (2011) concluded that, based on field relationships, the eruption of Purvine Hills is younger than Twin Mountain.

The pace of volcanism between approximately 62 and 37 ka differs from the earlier pulse of late Quaternary volcanism. Five eruptions between 61.7±1.1 ka and 36.6±2.3 ka yields an average eruption frequency of 1 event per 5 ky, a rate that is more than an order of magnitude greater than the earlier pulse of activity. Repose periods during this youngest pulse of activity are 7.5±2.1, 9.4±2.8, 8.1±3.2, and 0.1±6.4 ky indicating no systematic increase or decrease in activity during this period. After the eruption of Purvine Hills, the field entered a period of inactivity that continues to the present day. Interestingly, the current ~37 ky hiatus in eruptions is similar in magnitude to both the hiatus prior to the last pulse of activity (i.e, the repose period between eruptions at The Crater and Malpie Mountain) as well as the long-term average eruption frequency during the time period investigated.

Temporal-Spatial Trends

New $^{40}Ar/^{39}Ar$ ages, when combined with some of the age determinations of Stroud (1997), document a previously unrecognized migration in volcanism during the Capulin pulse of activity in the Raton-Clayton volcanic field (Fig. 5). Beginning at approximately 1.3 Ma and lasting until ~740 ka, volcanic activity was largely focused south to southeast of Raton between Eagle Tail Mesa (vent 11 of Table 2 and Fig. 5) and west of Horseshoe crater (vent 8 of Table 2 and Fig. 5). During this pulse, vents erupted along the western margin of the field and had no apparent vent migration patterns. Activity since 370 ka produced vents east of this earlier pulse, culminating in four eruptions near Capulin Volcano. The average migration rate, between 1.3 Ma and 37 ka, is 2.3 cm/yr eastward (Figs. 5A, B), with no systematic migration in latitude (Fig. 5C). Prior to ~1.3 Ma, there is limited evidence for any eastward vent migration trend during the Capulin phase. For example, the 1.7 Ma Mud Hill tuff cone (this study) is a less than 3 km from Capulin.

An alternative to calculating an average migration trend during the last 1.3 Ma of RCVF activity is to assess just the youngest series of eruptions. If only vents younger than 100 ka are used to determine migration characteristics, a somewhat different pattern emerges. Six vents (i.e., The Crater and younger; Fig. 5 and Table 2) define a NE migration rate of 65.9 cm/yr (calculated by quadratically summing the easting and northing vectors – dashed lines of Figs. 5A–C). Although both methods of characterizing the migration patterns demonstrate a general eastward migration of volcanism, the youngest six eruptions migrate at much greater rate to the northeast rather than in a general eastward direction. The calculated migration rates using different temporal windows (17 vents <1.3 Ma versus only the 6 that are <100 ka), as well as corresponding different eruption frequencies, demonstrate that short-term pulses of activity may vary, perhaps significantly, from the long-term characteristics of the field.

Questions arise regarding the newly discovered migration trends: *What is the cause of the migration in vent location? Why does the pattern of migration appear to only begin at 1.3 Ma?* Although a complete discussion of these questions is beyond the scope of this paper, some comments are briefly provided. Three geologic processes are typically invoked to explain volcanic vent migration: plate motion over a fixed mantle source (Condit et al., 1989; Tanaka et al., 1989; Crumpler et al., 1994), melting along and erosion of the lithospheric keel (Best and Brimhall, 1974; Crow et al., 2011), or extension that induces fracture propagation/dilation within the lithosphere (Warner, 1978; Panter et al., 1994; Fleck et al., 2014). Tanaka et al. (1989) and Condit et al. (1989) described vent migration patters of 2-3 cm/yr to the east-northeast for the late Cenozoic San Francisco and Springerville volcanic fields of Arizona, respectively, which they concluded was caused by the southwest motion of the North American plate over a fixed mantle source. The style of volcanism and vent migration in the RCVF is similar to both the aforementioned fields, but with one significant difference. Whereas migration at the San Francisco and Springerville fields was persistent during the lifespan of both of these fields (5.0 to < 0.1 Ma and ~2.1 to 0.5 Ma, respectively), migration of volcanism within the RCVF only started at ~1.3 Ma or 7.9 Ma after the initiation of activity within the field. Crow et al. (2011) and van Wijk et al. (2010) proposed that infiltration of the asthenosphere during the late Cenozoic initiated erosion of and melting along the base of the lithospheric mantle below the Colorado plateau. Both studies used large datasets of published geochronology to show that most volcanic fields adjacent to the margin of the plateau define migration trends toward the center of the plateau. In particular, Crow et al., (2011) suggested a field-wide westward migration of volcanism in the RCVF, which is nearly completely opposite to our proposed <1.3 Ma eastward migration trend, potentially signifying irregular migration patterns during the history of the RCVF. Lastly, fracture propagation could explain some of the observed trends in migration in the RCVF. The eastward migration of volcanism is sub-parallel to the NE-trending Jemez lineament, suggesting some structural control. If migration of volcanism is somehow related to dilation of deep-seated structures within the Jemez lineament that permit melt segregation, emplacement, and eruption of magmas, what caused the systematic extension or change in stress orientation to begin at ~1.3 Ma? Work is now focused on resolving how each of these mechanisms may play a role, perhaps at different periods during the lifespan of the RCVF, in the observed vent migration trends within the field.

CONCLUSIONS WITH IMPLICATIONS FOR VOLCANIC HAZARDS

New ^{40}Ar/^{39}Ar ages, combined with pre-existing geochronology, provide insights into the timescale and hazards of late Quaternary volcanism associated with the Raton-Clayton volcanic field. New ages determined as part of this study indicate that nine vents erupted between 368.2±7.3 and 36.6±6.0 ka. Volcanism during this period is characterized by early eruptions from geographically dispersed vents with significant repose periods of more than 100 ka. Between 61.7±1.1 and 36.6±6.0 ka five vents erupted at an average frequency of 1 event per 5 ky ,with irregular repose periods. Although similar rates of activity likely occurred during the 9.2 Ma lifespan of the field, results indicate the pace of volcanism increased during the late Quaternary. Given the longevity of the eruptive history in the Raton-Clayton field and evidence that long periods of inactivity are followed by pulses of sustained activity, the current eruptive hiatus of ~37 ky is not interpreted to represent the full cessation of volcanic activity at the northeast limit of the Jemez lineament. Instead, future volcanic activity is highly likely, despite the current inactivity in the field. In addition to the newly determine rates of activity, this study also identified an eastward vent migration pattern, starting at ~1.3 Ma along the western margin of the field and tracking to the youngest eruptions near Capulin. Although volcanic activity is notoriously unpredictable and a vent may erupt at any location within the field, if the next eruption follows similar patterns of migration during the last 1.3 Ma, the vent may be located near Capulin Volcano, and perhaps further to the east or northeast. Regardless of when and where the next eruption(s) will occur, hazard planning for northeastern New Mexico, and New Mexico in general, should include protocols for an eruption scenario.

ACKNOWLEDGMENTS

This project was funded by NSF grant EAR-1322089 and by the New Mexico Bureau of Geology and Mineral Resources. Special thanks to Capulin Volcano National Monument for allowing access to collect samples within the park boundary. Matt Heizler, Jake Ross, Bill McIntosh, and Lisa Peters provided help during the laboratory analyses and, along with Frank Ramos, provided invaluable feedback for many of the ideas presented in the paper. Reviews by Jake Ross and Larry Crumpler greatly improved the manuscript.

REFERENCES

Baldwin, B., and Muehlberger, W., 1959, Geologic studies of Union County, New Mexico: NM Bureau of Mines and Mineral Resources Bulletin 63, 171 p.

Best, M.G., and Brimhall, W.H., 1974, Late Cenozoic alkalic basaltic magmas in western Colorado Plateaus and Basin and Range transition zone, USA, and their bearing on mantle dynamics: Geological Society of America Bulletin, v. 85, p. 1677-1690.

Chapin, C.E, Wilks, M., and McIntosh, W.C., 2004, Space-time patters of Late Cretaceous to present magmatism in New Mexico-comparison with Andean volcanism and potential for future volcanism: New Mexico Bureau of Geology and Mineral Resources, Bulletin 160, p. 13-40.

Condit, C. D., Crumpler, L.S., Aubele, J.C., and Elston, W.E., 1989, Patterns of volcanism along the southern Margin of the Colorado Plateau: The Springerville field: Journal of Geophysical Research, v. 94, p. 7975-7986.

Crow, R., Karlstrom, K., Asmerom, Y., Schmandt, B., Polyak, V., and DuFrane, S.A., 2011, Shrinking of the Colorado Plateau via lithospheric mantle erosion: Evidence from Nd and Sr isotopes and geochronology of Neogene basalts: Geology, v. 39, p. 27-30.

Crumpler, L.S., Aubele, J.C., and Condit, C.D., 1994, Volcanoes and neotectonic characteristics of the Springerville volcanic field, Arizona: New Mexico Geological Society, Guidebook 45, p. 147-164.

Fleck, R.J., Sutter, J.F., Elliot, D.H., 1977. Interpretation of discordant ^{40}Ar/^{39}Ar age-spectra of Mesozoic tholeiites from Antarctica: Geochimica Cosmochimica Acta, v. 41, p. 15-32.

Fleck, R.J., Hagstrum, J.T., Calvert, A.T., Evarts, R.C. and Conrey, R.M., 2014, ^{40}Ar/^{39}Ar geochronology, paleomagnetism, and evolution of the Boring volcanic field, Oregon and Washington, USA: Geosphere, v. 10, p. 1283-1314.

Hoffer, J.M., and Corbitt, L.L., 1991, Evolution of the Late Cenozoic Jornada volcano, south-central New Mexico: New Mexico Geological Society, Guidebook 42, p. 159-163.

Karlstrom, K.E., and Bowring, S.A., 1988, Early Proterozoic assembly of tectonostratigraphic terranes in southwestern North America: Journal of Geology, v. 96, p. 561-576.

Kelley, V.C., and Kudo, A.M., 1978, Volcanoes and related basalts of Albuquerque Basin, New Mexico: New Mexico Bureau of Mines and Mineral Resources, Circular 156, 30 p.

Koppers, A.A.P., Staudigel, H., and Wijbrans, J.R., 2000, Dating crystalline groundmass separates of altered Cretaceous seamount basalts by the 40Ar/39Ar incremental heating technique: Chemical Geology, v. 166, p. 139-158.

Kuiper, K.F., Deino, A., Hilgen, F.J., Krijgsman, W., Renne, P.R., and Wijbrans, J.R., 2008, Synchronizing rock clocks of earth history: Science, v. 320, p. 500-504.

Neir, A.O., 1950, A redetermination of the relative abundances of the isotopes of carbon, nitrogen, oxygen, argon, and potassium: Physical Review Letters, v. 77, p. 789-793.

Nereson, A., Stroud, J., Karlstrom, K., Heizler, J., and McIntosh, W., 2013, Dynamic topography of the western Great Plains: Geomorphic and ^{40}Ar/^{39}Ar evidence for mantle driven uplift associated with the Jemez lineament of NE New Mexico and SE Colorado: Geosphere, v. 9, p. 1-25.

Panter, K.S., McIntosh, W.C., and Smellie, J.L., 1994, Volcanic history of Mount Sidley, a major alkaline volcano in Marie Byrd Land, Antarctica: Bulletin of Volcanology, v. 56, p. 361-376.

Sayre, W.O., and Ort, M.H., 2011, A geologic study of the Capulin Volcano National Monument and surrounding areas, Union and Colfax Counties, New Mexico: New Mexico Bureau of Geology and Mineral Resources, Open-file Report 541, 71 p.

Sayre, W.O., Ort, M.H., and Graham, D., 1995, Capulin Volcano is approximately 59,100 years old: cosmogenic helium aging technique key to clearing up age old question: Park Science, v. 15, p. 10-11.

Scholle, P.A., 2003, Geologic Map of New Mexico: New Mexico Bureau of Geology and Mineral Resources, scale 1:500,000.

Scott, G.R., Wilcox, R.E., and Mehnert, H.H., 1990, Geology of volcanic and subvolcanic rocks of the Raton-Springer area, Colfax and Union Counties, New Mexico: U.S. Geological Survey, Professional Paper 1507, 68 p.

Stormer, J.C., 1972, Ages and nature of volcanic activity on the Southern High Plains, New Mexico and Colorado: Geological Society of America Bulletin, v. 83, p. 2443-2448.

Stroud, J.R., 1997, Geochronology of the Raton-Clayton volcanic field, with implications for volcanic history and landscape evolution [MS thesis]: Socorro, New Mexico Institute of Mining and Technology, 102 p.

Tanaka, K.L., Shoemaker, E.M., Ulrich, G.E., and Wolfe, E.W., 1986, Migration of volcanism in the San Francisco volcanic field, Arizona: Geological Society of America Bulletin, v. 97, p. 129-141.

van Wijk, J.W., Baldridge, W.S., van Hunen, J., Goes, S., Aster, R., Coblentz, D.D., Grand, S.P., and Ni, J., 2010, Small-scale convection at the edge of the Colorado Plateau: Implications for topography, magmatism, and evolution of Proterozoic lithosphere: Geology, v. 38, p. 611-614.

Warner, L.A., 1978, The Colorado Lineament: A middle Precambrian wrench

fault system: Geological Society of America Bulletin, v. 89, p. 161-171.
Williams, W.J.W., 1999, Evolution of Quaternary intraplate mafic lavas detailed using ^{3}He surface exposure and $^{40}Ar/^{39}Ar$ dating, and elemental and He, Sr, Nd, and Pb isotopic signatures; Potrillo volcanic field, New Mexico, U.S.A. and San Quintin volcanic field, Baja California Norte Mexico [Ph.D. dissertation]: El Paso, University of Texas, 195 p.
York, D., 1969, Least squares fitting of a straight line with correlated errors: Earth and Planetary Science Letters, v. 5, p. 320-324.

Supplemental data can be found at http://nmgs.nmt.edu/repository/index.cfml?rid=2019003